

Enhanced Signal Detection for Massive SIMO Communications with 1-Bit ADCs

Doaa Abdelhameed^{1,2}, Kenta Umabayashi¹, Ahmed Al-Tahmeesschi¹, Italo Atzeni³, and Antti Tölli³

¹Graduate School of Engineering, Tokyo University of Agriculture and Technology, Japan

²Dept. of Electrical Engineering, Aswan University, Egypt

³Centre for Wireless Communications, University of Oulu, Finland

Abstract—This paper considers a massive single-input single-output (SIMO) system with 1-bit analog-to-digital converters (ADCs) at the base station (BS). In this context, the stochastic resonance phenomenon can be exploited together with the massive number of antennas to enable the symbol detection. In this regard, we investigate the statistics of the estimated symbols when maximum ratio combining (MRC) is adopted at the BS. In addition, assuming 16 quadrature amplitude modulation (16-QAM), we propose three different symbol detectors that are designed based on the mean and variance of the MRC outputs. Through numerical evaluations, we show that the proposed symbol detectors can significantly enhance the symbol error rate performance of massive SIMO systems with 1-bit ADCs.

Index Terms—Massive SIMO, 1-bit ADCs, MRC, Data detection

I. INTRODUCTION

Massive multiple-input multiple-output (MIMO) is one of the key technologies of current and future mobile systems, whereby the base stations (BS) are equipped with a large number of antennas [1]. Massive MIMO enables enormous gains in terms of spectral efficiency and reliability [2]. However, using a massive antenna array at the BS leads to an increase in both hardware complexity and power consumption, which hinders its practical implementation [3]. In this regard, using low-resolution analog-to-digital/digital-to-analog converters (ADCs/DACs) to quantize the received/transmitted signals (down to 1-bit) has gained attention as a promising solution for these practical impediments.

Several recent works have considered the impact of 1-bit ADCs on the performance of massive MIMO systems. The performance loss in terms of the capacity due to the 1-bit quantization has been quantified in [4], [5], and [6] that amounts about 36% in the low signal-to-noise ratio (SNR) regime compared with the ideal full-resolution ADCs

The work of D. Abdelhameed was supported by the Ministry of Higher Education of the Arab Republic of Egypt. The work of K. Umabayashi was supported by the European Commission in the framework of the H2020-EUJ-02-2018 project 5GEnhance (Grant agreement no. 815056), by “Strategic Information and Communications R&D Promotion Programme (SCOPE)” of Ministry of Internal Affairs and Communications (MIC) of Japan (Grant no. JPJ000595), the JSPS KAKENHI Grant Numbers JP18K04124 and JP18KK0109, Institute of Global Innovation Research in TUAT. The work of I. Atzeni was supported by the Marie Skłodowska-Curie Actions (MSCA-IF 897938 DELIGHT). The work of A. Tölli was supported by the Academy of Finland under grant no. 318927 (6Genesis Flagship).

case. The study in [7] utilized the Bussgang decomposition, which allows to reformulate the nonlinear 1-bit quantization as a linear function, to design a channel estimator called Bussgang linear minimum mean squared error (BLMMSE). The authors in [8] extended the study in [7] for a non-zero-threshold quantizer providing a generalized BLMMSE as well as investigating a quantizer threshold design. In [9], a near maximum-likelihood (ML) detector and ML channel estimator were suggested for the massive MIMO system with 1-bit ADCs. For the multi user MIMO orthogonal frequency division multiplexing system with 1-bit ADC, the authors in [10] investigated a nonlinear data detection approach and developed its corresponding very large scale integration design. The uplink achievable rate and symbol error rate (SER) for 1-bit quantized massive MIMO systems were considered in [11]. Here, the authors used a simple linear receiver (zero-forcing (ZF) or maximum ratio combining (MRC)) and linear channel estimation (least-squares (LS)) for quadrature phase-shift key (QPSK) modulation.

In case of higher-order modulation schemes, such as 16 quadrature amplitude modulation (16-QAM), 1-bit ADCs for the in-phase and quadrature components do not have enough degrees of freedom for appropriate demodulation in the case of single antenna at the BS. However, as an extension of [11], the performance evaluation of the 1-bit quantized massive MIMO system with 16-QAM modulation was presented in [12]. Here, the authors showed that a massive number of antennas at the BS can help in detecting 16-QAM signal phase and amplitude with simple linear receiver (MRC, ZF) after coarsely quantizing the received signal at the BS. The authors in [13] studied the constructive noise phenomenon (also known as stochastic resonance [14]) observed in detecting 16-QAM signal in 1-bit ADCs based single-input multi-output (SIMO) system. In this case, the degrees of freedom given by the multiple antennas and the constructive noise phenomenon can slightly enhance the performance of the 16-QAM signal detection in terms of SER. Recently, the authors in [15] provided closed-form expressions of the expected value and the variance of the estimated symbols when MRC is adopted at the BS along with their asymptotic behavior at high SNR.

In this paper, we propose three symbol detectors in case of the massive SIMO system with 1-bit ADCs. The main contributions of this paper are summarized as follows.

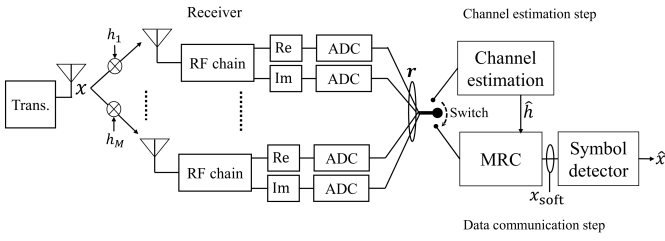


Fig. 1. System Model.

- 1) We investigate the statistics of the MRC outputs for massive SIMO reception. The distribution shape of the MRC outputs for a certain transmitted symbol is an ellipse rather than a circle. This investigation reveals that the conventional symbol detector is not appropriate in this case.
- 2) We propose three symbol detectors based on the statistics of the MRC outputs for the massive SIMO reception. Specifically, mean and variance of the MRC outputs, in addition, the distribution of variance in the I-Q plane are considered in the proposed symbol detectors.
- 3) Through numerical evaluations, we show the benefits of the proposed detectors in terms of SER against the conventional detector. In this regard, the statistics considered in the proposed detectors are characterized by different gains.

The rest of the paper is organized as follows. The system setup and the problem formulation are presented in Section II. The proposed symbol detectors are shown in Section III. In Section IV, the proposed schemes are validated through numerical results, while Section V concludes the paper.

Notation: we refer to the matrices and vectors with boldface uppercase and lowercase letters, respectively, and both A , a represent scalar symbols. $a_{m,n}$ represents the (m,n) th element of a matrix and a_m is the m th element of a vector. $\Re(\cdot)$ and $\Im(\cdot)$ denote the real and imaginary parts of a complex number, respectively. Furthermore, $(\cdot)^H, (\cdot)^*$, $(\cdot)^T$ and \mathbf{I} denotes a Hermitian transpose of a matrix, a conjugate operator, transpose of a matrix, and identity matrix, respectively.

II. SYSTEM MODEL

In this paper, the uplink single cell large-scale SIMO system where the BS equipped with M antennas serving a single user (UE) is considered. The considered system model is shown in Fig. 1. Each BS antenna attached with 1-bit ADCs pair for in-phase and quadrature phase received symbol components (i.e., $2M$ quantizers are required at the BS). We assume block fading channel and the channel coefficient for each antenna is denoted by h_m and the channel coefficient vector between the UE and M antennas at the BS is denoted by $\mathbf{h} \in \mathbb{C}^{M \times 1}$ in which $h_m \sim \mathcal{CN}(0,1)$ and each h_m is identical independent distributed (i.i.d.). The equivalent baseband model is assumed.

In the procedure at the BS, there are two steps: channel estimation step and data communication step. In the channel estimation step, the UE transmits a pilot sequence $\mathbf{x}_p \in \mathbb{C}^{1 \times P}$

as a training sequence to estimate the channel vector where P indicates the number of symbols for the pilot sequence.

The baseband received pilot sequence at the BS is given by

$$\mathbf{Y}_p = \mathbf{h}\mathbf{x}_p + \mathbf{N}_p, \quad (1)$$

where $\mathbf{Y}_p \in \mathbb{C}^{M \times P}$, and $\mathbf{N}_p \in \mathbb{C}^{M \times P}$ is the additive white Gaussian noise (AWGN) matrix with elements distributed as $\mathcal{CN}(0, \sigma_p^2)$. The vector of the 1-bit ADCs outputs for the received pilot symbols is given as

$$\mathbf{R}_p = Q(\mathbf{Y}_p) = \text{sgn}(\Re(\mathbf{Y}_p)) + j\text{sgn}(\Im(\mathbf{Y}_p)) \quad (2)$$

where sgn is the element-wise signum function, i.e.,

$$\text{sgn}(s) = \begin{cases} -1, & \text{if } s < 0. \\ 1, & \text{otherwise.} \end{cases} \quad (3)$$

In the channel estimation step, we obtained the estimated channel vector as follows,

$$\hat{\mathbf{h}} = \frac{\mathbf{R}_p \mathbf{x}_p^H}{\mathbf{x}_p \mathbf{x}_p^H}, \quad (4)$$

where the entries of \mathbf{R}_p will be one of 4 possible candidates (i.e., the 1-bit ADCs possible outputs) and the LS estimation output (i.e., \hat{h}_m) will have one of 4^P possible values. Assuming a static channel during a coherence time T , i.e., block fading channel, where the first P samples are occupied by the pilot symbols and the remaining $T_d = T - P$ samples are occupied by the UE data symbols.

In the data communication step, the received symbols at the BS is given as

$$\mathbf{y} = \mathbf{h}\mathbf{x} + \mathbf{n}, \quad (5)$$

where $\mathbf{y} \in \mathbb{C}^{M \times 1}$ is the received signal vector, x is the transmitted symbol, $\mathbf{n} \in \mathbb{C}^{M \times 1}$ is AWGN vector with elements distributed as $\mathcal{CN}(0, \sigma_n^2)$. For the transmitted signals x and \mathbf{x}_p , 16-QAM is used for the modulation scheme while higher-order QAM is also applicable in this work.

The output vector of the 1-bit ADCs is given by

$$\mathbf{r} = \text{sgn}(\Re(\mathbf{y})) + j\text{sgn}(\Im(\mathbf{y})). \quad (6)$$

Utilizing the estimated channel vector $\hat{\mathbf{h}}$, the soft estimation x_{soft} of x based on MRC is obtained as

$$x_{\text{soft}} = \frac{\hat{\mathbf{h}}^H \mathbf{r}}{\|\hat{\mathbf{h}}\|^2}. \quad (7)$$

As shown in Fig. 1, the detection result \hat{x} is given by a symbol detection of x_{soft} . In this paper, three symbols detectors are investigated to consider the effect of the 1-bit ADCs at x_{soft} . In addition, the typical detector for M-ary QAM signal [9] is mentioned for comparison.

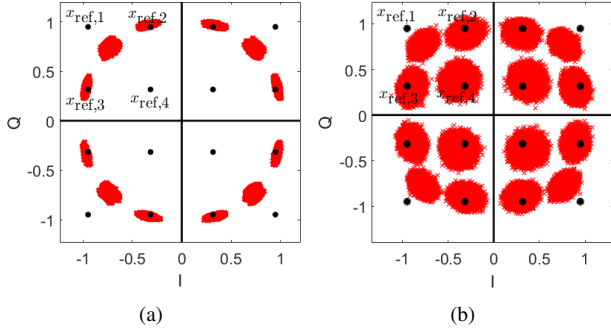


Fig. 2. The MRC output of 1x400 SIMO system, with $P = 20$. (a) high SNR Case, $SNR = 20dB$ (b) low SNR Case, $SNR = 0dB$.

III. SYMBOL DETECTORS

In Fig. 2, the MRC outputs (x_{soft}) in the I-Q plane are plotted. The result in Fig. 2(a) is in high SNR (20 dB), on the other hand the SNR in Fig. 2(b) corresponds to low SNR (0 dB). In both cases, $M = 400$ and $P = 20$. The black dots in the figure correspond to the 16-QAM constellations in the I-Q plane. These symbols are denoted by $x_{\text{ref},k}$ and k ($1 \leq k \leq 16$) is the index number for each constellation point. The result in high SNR (Fig. 2(a)) indicates that the 1-bit ADCs do not have enough degrees of freedom to detect 16-QAM signal adequately. Specifically, the received signals from $x_{\text{ref},1}$ and $x_{\text{ref},4}$ cannot be recognized since they are overlapped. On the other hand, the result at low SNR (Fig. 2(b)) indicates that thanks to the stochastic resonance phenomenon due to the noise component \mathbf{n} [14] and massive number of antennas, the 16-QAM signal can be detectable.

A. Conventional Symbol Detector

In the conventional symbol detector, the detection result is given by

$$\hat{x} = \arg \min_{x_{\text{ref},k}} \|x_{\text{soft}} - x_{\text{ref},k}\|. \quad (8)$$

In this detector, the typical constellations (black dot in Fig. 2) are used as the reference position in the I-Q plane. The distributions of actual received signals in Fig. 2 indicate that the reference does not fit the actual received signals. For this issue, the proposed symbol detectors consider the distribution of the actual received signals. Specifically, at first, statistics of x_{soft} are obtained and the proposed symbol detectors are shown later.

B. Statistics of x_{soft}

The statistics of x_{soft} under $x_{\text{ref},k}$ is used to design the symbol detectors. The mean of x_{soft} under $x_{\text{ref},k}$ is defined by

$$\mu_k = E[x_{\text{soft}} | x_{\text{ref},k}], \quad (9)$$

where $E[\cdot]$ is the expectation operator in terms of \mathbf{n} and \mathbf{h} .

In Figs. 3(a) and 3(b), the real and imaginary parts of μ_k where $k = 1, 2, 3$ and 4 are plotted as a function of SNR, respectively. These results reveal that μ_1 and μ_4 get close

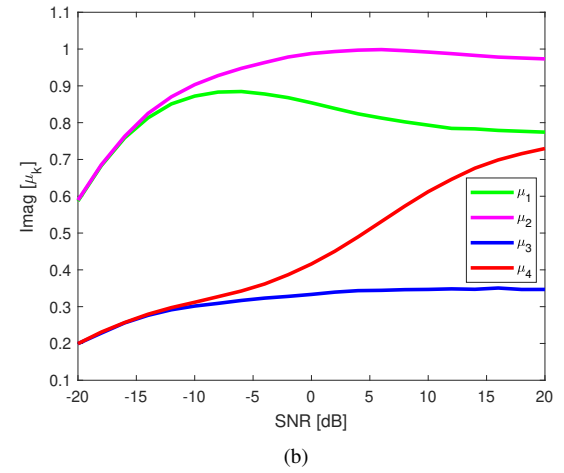
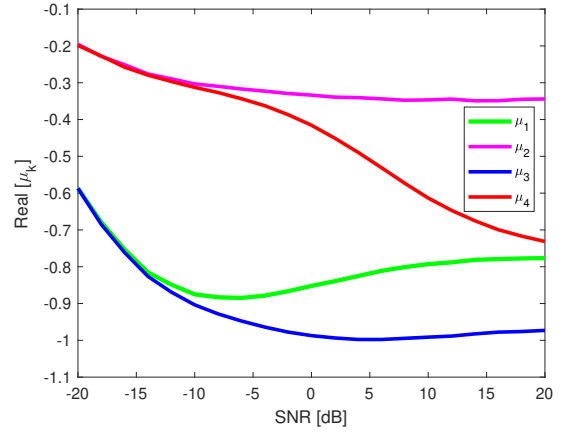


Fig. 3. The μ_k as a function of SNR. (a) Real part, (b) Imaginary part.

as SNR increases. This behavior can be confirmed also in Fig. 2(a). On the other hand, in low SNR region, such as less than 0 dB, each μ_k located apart from each other.

In Fig. 4, the distribution of x_{soft} (red star) under $x_{\text{ref},1}$ is plotted. The contour of distribution is an ellipse rather than a circle, and this shape depends on $x_{\text{ref},k}$ as confirmed in Fig. 2(b). In addition, the variance of x_{soft} also depends on the direction from μ_k . Therefore, we define two types of variances for x_{soft} . The typical variance of x_{soft} , which is averaged over all directions, is defined by

$$\sigma_k^2 = E[(x_{\text{soft}} - \mu_k)(x_{\text{soft}} - \mu_k)^* | x_{\text{ref},k}]. \quad (10)$$

The variance of x_{soft} in terms of the direction θ that is defined in Fig. 4 is obtained by

$$\sigma_k^2(\theta) = E[(\exp(j\theta)(x_{\text{soft}} - \mu_k)^* \cdot (\exp(j\theta)(x_{\text{soft}} - \mu_k)^*)^* | x_{\text{ref},k})]. \quad (11)$$

In this variance, the distribution of x_{soft} on the direction of $\exp(j\theta)$ in the I-Q plane is considered as shown in Fig. 4. For the direction θ , the reference vector \mathbf{x}_r is set to

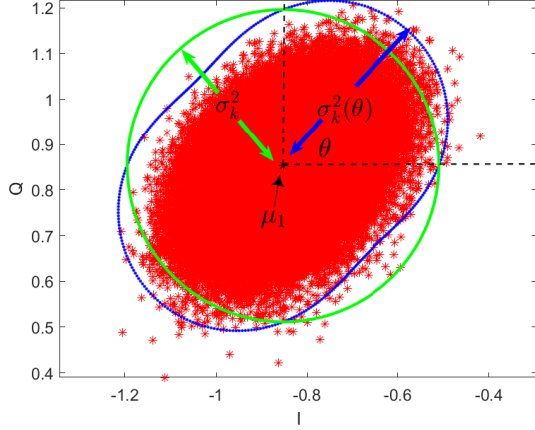


Fig. 4. Angle-based variance estimation validation for 1-bit ADCs 1x100 SIMO system, $SNR = 0dB$.

$[\cos(\theta), \sin(\theta)]^T$. Let \mathbf{x} be a vector from μ_k to x_{soft} in the I-Q plane. The variance $\sigma_k^2(\theta)$ corresponds to the variance of the orthogonal projections of \mathbf{x} along \mathbf{x}_r .

C. Mean-Based Symbol Detector

As we confirmed in Fig. 2, $x_{\text{ref},k}$ and μ_k are significantly different. In this proposed symbol detector, μ_k is used for symbol detection. The detection result based on mean-based symbol detector is given by

$$\hat{x} = \arg \min_{x_{\text{ref},k}} \|x_{\text{soft}} - \mu_k\|, \quad (12)$$

where μ_k is a function of $x_{\text{ref},k}$ according to (9).

D. Mean and Averaged Variance-Based Symbol Detector

From Fig. 2, the distribution of x_{soft} depends on not only the mean but also variance. In this second proposed symbol detector, μ_k and averaged variance σ_k^2 are used for symbol detection. The detection rule is given by

$$\hat{x} = \arg \min_{x_{\text{ref},k}} \frac{\|x_{\text{soft}} - \mu_k\|}{\sqrt{\sigma_k^2}}, \quad (13)$$

where the square root of the variance is used for the normalization.

E. Mean and Direction-Oriented Variance-Based Symbol Detector

The distributions in Fig. 2 reveal that the variance depends on the direction θ_k . In the mean and direction oriented variance-based symbol detector, the variance for the direction and mean are used for symbol detection as

$$\hat{x} = \arg \min_{x_{\text{ref},k}} \frac{\|x_{\text{soft}} - \mu_k\|}{\sqrt{\sigma_k^2(\theta_k)}}. \quad (14)$$

Fig. 5 provides an intuitive understanding of this symbol detector. In this example, the received signal locates at the point with x_{soft} . Each ellipse indicate the magnitude of the variances for all directions from μ_k . In this detector, the variance from μ_k to x_{soft} are selected, such as $\sigma_1^2(\theta_1)$ and $\sigma_2^2(\theta_2)$ in this figure, for the normalization in (14).

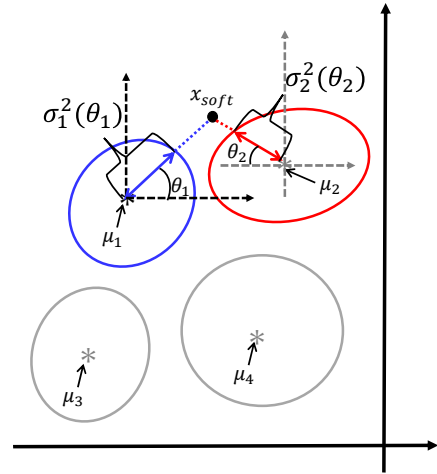


Fig. 5. Mean and direction oriented variance-based symbol detection in I-Q plane.

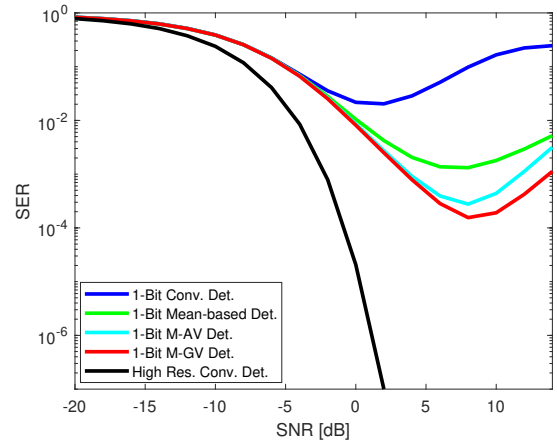


Fig. 6. SER as a function of SNR for conventional symbol detector, three proposed symbol detector, and high-resolution ADCs performances. $P = 256$ and $M = 100$.

IV. NUMERICAL EVALUATION

In this section, we compare the four symbol detectors, conventional symbol detector, mean-based symbol detector, mean and average variance-based symbol detector, and mean and direction oriented variance-based symbol detector. They are evaluated based on SER performance.

Fig. 6 shows the SER versus the SNR for $M = 100$. The pilot length is set to $P = 256$. In this result, we also show the SER performance of high-resolution ADCs for comparison. The proposed three detectors exhibit a significant improvement in terms of SER compared with the conventional detector (1-Bit Conv. Det.). The gap between the conventional detector and the mean-based symbol detector (1-Bit Mean-based Det.) shows a gain due to the use of μ_k as a reference point. This gain is the most significant compared to the other statistics σ_k^2 and $\sigma_k^2(\theta_k)$. The gap between the mean-based symbol detector and the mean and average variance-based symbol detector (1-

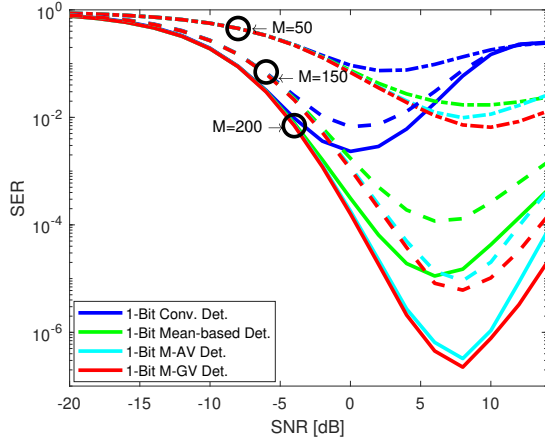


Fig. 7. SER as a function of SNR for conventional symbol detector, three proposed symbol detector, and high-resolution ADCs performances. $P = 256$ and $M = 50, 150,$ and 200 .

Bit M-AV Det.) indicates the gain due to σ_k^2 . Finally, the gap between the mean and average variance-based symbol detector and the mean and direction oriented variance-based symbol detector (1-Bit M-GV Det.) shows the gain due to the variance for direction θ_k .

In the 1-bit ADCs cases, there are optimum SNRs that can minimize SER while the high-resolution ADCs do not have the optimum SNR. In addition, the optimum SNR depends on the symbol detector, such as the optimum SNR for mean and direction oriented variance-based symbol detector is about 8 dB. This results indicates that high SNR is not always good for 1-bit ADCs with 16-QAM or higher modulation scheme. This can be also confirmed from the result in Figs. 2(a) and 2(b). Specifically, the received signals from $x_{\text{ref},1}$ and $x_{\text{ref},4}$ get closer to each other for the high SNR case due to the distortion in 1-Bit ADC. This fact indicates that measures for the distortion at both transmitter and receiver sides are required. This work focuses on the symbol detector at the receiver side. The gap between the high-resolution ADCs and the proposed methods is still significant and there is optimum SNR. These indicate that additional measure at the transmitter side is required.

Fig. 7 shows the SER performances for the symbol detectors with different antenna numbers, i.e., $M = 50$, $M = 150$, and $M = 200$. For all methods, as expected, increasing the number of antennas is beneficial. The gain in the conventional symbol detector is the smallest among all symbol detectors. Specifically, the gains due to M with μ_k and/or σ_k^2 are more significant than the gain due to θ_k in $\sigma_k^2(\theta_k)$. In addition, the results indicate that the optimum SNR also depends on M .

V. CONCLUSION

In this paper, three symbol detectors for massive SIMO communication systems with 1-bit ADCs and M -ary QAM modulation have been investigated. The distribution of the MRC outputs in the I-Q plane has implied that the conventional symbol detector may not be appropriate for the signal

detection in systems with 1-bit ADCs. For this issue, we obtain the statistics of the distribution of the MRC outputs empirically, and proposed three symbol detectors. In addition, we compared the proposed three schemes with the conventional detector. Numerical evaluations have revealed that the proposed symbol detectors can achieve significantly better SER performance than the conventional symbol detector in the case of 1-bit quantized massive SIMO systems. The utilization of the statistics, such as mean and variance of MRC outputs, and direction oriented variance can provide reasonable gains in the SER performances. However, SER of the high-resolution ADCs based symbol detector is much less than SER of the proposed methods. Therefore, further improvement may be expected by a modification of constellation in the transmitted symbols and this is one of the future works.

REFERENCES

- [1] E. G. Larsson, O. Edfors, F. Tufvesson, and T. L. Marzetta, "Massive MIMO for next generation wireless systems," *IEEE Commun. Mag.*, vol. 52, no. 2, pp. 186–195, Feb. 2014.
- [2] E. Björnson, E. G. Larsson, and M. Debbah, "Massive MIMO for maximal spectral efficiency: How many users and pilots should be allocated?" *IEEE Trans. Wireless Commun.*, vol. 15, no. 2, pp. 1293–1308, Feb. 2016.
- [3] R. Chataut and R. Akl, "Massive MIMO systems for 5G and beyond networks—Overview, recent trends, challenges, and future research direction," *Sensors*, vol. 20, no. 10, p. 2753, May 2020.
- [4] M. S. Stein, S. Bar, J. A. Nossek, and J. Tabrikian, "Performance analysis for channel estimation with 1-Bit ADC and unknown quantization threshold," *IEEE Trans. Signal Process.*, vol. 66, no. 10, p. 2557–2571, May 2018.
- [5] A. Mezghani and J. A. Nossek, "On ultra-wideband MIMO systems with 1-bit quantized outputs: Performance analysis and input optimization," in *Proc. IEEE Int. Symp. Inf. Theory (ISIT)*, Jun. 2007.
- [6] —, "Analysis of 1-bit output noncoherent fading channels in the low SNR regime," in *Proc. IEEE Int. Symp. Inf. Theory (ISIT)*, Jun. 2009.
- [7] Y. Li, C. Tao, G. Seco-Granados, A. Mezghani, A. L. Swindlehurst, and L. Liu, "Channel estimation and performance analysis of one-bit massive MIMO systems," *IEEE Trans. Signal Process.*, vol. 65, no. 15, p. 4075–4089, Aug. 2017.
- [8] Q. Wan, J. Fang, Z. Chen, and H. Li, "Generalized Bussgang LMMSE channel estimator for one-bit massive MIMO systems," in *Proc. IEEE Global Commun. Conf. (GLOBECOM)*, Dec. 2019.
- [9] J. Choi, J. Mo, and R. W. Heath, "Near maximum-likelihood detector and channel estimator for uplink multiuser massive MIMO systems with one-bit ADCs," *IEEE Trans. Commun.*, vol. 64, no. 5, pp. 2005–2018, May 2016.
- [10] S. H. Mirfarshbafan, M. Shabany, S. A. Nezamalhosseini, and C. Studer, "Algorithm and VLSI design for 1-bit data detection in massive MIMO-OFDM," *IEEE open j. circuits syst.*, vol. 1, pp. 170–184, 2020.
- [11] C. Risi, D. Persson, and E. G. Larsson, "Massive MIMO with 1-bit ADC," Apr. 2014. [Online]. Available: <http://arxiv.org/abs/1404.7736>
- [12] S. Jacobsson, G. Durisi, M. Coldrey, U. Gustavsson, and C. Studer, "One-bit massive MIMO: Channel estimation and high-order modulations," in *Proc. IEEE Int. Conf. Commun. Workshops (ICCW)*, Jun. 2015.
- [13] L. Liu, Y. Ma, and R. Tafazolli, "MIMO or SIMO for wireless communications with binary-array receivers," in *Proc. IEEE Int. Conf. Commun. Workshops (ICCW)*, Jun. 2020.
- [14] S. Kay, "Can detectability be improved by adding noise?" *IEEE Signal Process. Lett.*, vol. 7, no. 1, pp. 8–10, Jan. 2000.
- [15] I. Atzeni and A. Tölli, "Uplink data detection analysis of 1-bit quantized massive MIMO," in *Proc. IEEE Int. Workshop Signal Process. Adv. in Wireless Commun. (SPAWC)*, Sep. 2021.